Indian Journal of Experimental Biology
Vol. 61, November 2023, pp. 819-832
DOI: 10.56042/ijeb.v61i11.3267

Antiproliferative potential of bioactive molecule from *Murraya koenigii* L. Spreng against breast cancer: *In vitro* and *in vivo* studies and gene expression analyses

Mullai Valli Ramamoorthy[1], Bhamare Deepak Prashant[1], Deepu Mathew[1,2]*†, Babu Thekkekara Devassy[3], Shylaja Muthangaparambil Raman[1], Pareeth Chennattu Muhammed[3] & Smita Nair[1]

[1]Centre for Plant Biotechnology and Molecular Biology; [2]Bioinformatics Centre, Kerala Agricultural University, Thrissur - 680 656, Kerala, India

[3]Department of Biochemistry, Amala Cancer Research Centre, Thrissur - 680 555, Kerala, India

Received 20 January 2023; *Revised 08 May 2023*

The curry leaf extract is known to have anticancer property against breast cancer. Identification of the specific compound therein the curry leaf and its validation is essential for successful discovery of drugs. In that content, here, we extracted oleoresin from the mature curry leaves was subjected to antioxidant fractionation using column chromatography. Fraction obtained using 60:40 hexane and ethyl acetate solvent system, showing the maximum inhibition of DPPH, was sub-fractionated and those with the highest antioxidant property was analyzed in LC-MS/MS. Spectrum of molecules identified, along with FDA approved drugs, were docked with target proteins for breast cancer. *In vitro* screening of candidate phytocompounds doxylamine, histidinol and pheniramine, in their commercially available form, through Trypan blue exclusion assay against murine cancer cell lines EAC and DLA had shown that they have no cytotoxicity. Pheniramine maleate salt (PMS), doxylamine succinate salt (DSS) and L-histidinol dihydrochloride (LHD) have shown dose-dependent inhibition of proliferation of MCF-7 cells, with 280 µg/mL PMS at 72 h of incubation giving the maximum of 98.46%. Acute toxicity studies in Swiss albino mice (100 mg PMS/kg body wt.) have confirmed that the drug has no toxicity. Mouse mammary pad tumour model has shown that PMS significantly reduces the WBC count in the tumour induced mice. Liver function tests, histopathological analyses of liver, mammary pad and kidney tissues and expression analysis of oncogenes *ER-α1*, *Bcl-2*, *c-Myc* and *Pin1* have confirmed the drug candidature of PMS.

Keywords: Antioxidant fraction, Drug design, Mammary tumour model, Molecular docking, Oncogene expression

Breast cancer is the cancer with the highest incidence globally, with 300,590 estimated new cases and 43,700 estimated deaths in 2023 in the United States. It accounts for 15.81% of total estimated new cases and 7.95% of total estimated cancer deaths, respectively[1,2]. In 2022, India recorded the estimated breast cancer incidences year of 2,21,757 in both the sexes[3]. The existing treatment strategies are surgery, radiation, hormone therapy, chemotherapy, targeted therapy, immunotherapy, photodynamic therapy and stem cell transplantation. Though these treatments are differentially successful to contain the progression of cancer, side effects such as infection, weakened immune system, bleeding, hair loss, nausea, vomiting, diarrhea and constipation, are common, especially from the chemicals used in chemotherapy. In the past few decades, there have been reports of resistance to synthesized drugs, resulting reduced efficacy and survival rates[4-6]. Hence, there is a demand for the identification of cancer drugs with no side effects.

Plants have been excellent sources for therapeutic molecules and many phytocompounds are being tested for their efficacy in treating various cancers. An efficient method of drug discovery, both in terms of cost and money, is *in silico* designing through homology modeling, molecular docking, virtual high-throughput screening, molecular dynamic simulation or microarray analysis[7].

*Correspondence:
Phone: +91 9446478503 (Mob.)
E-Mail: deepu.mathew@kau.in;
†ORCID: https://orcid.org/0000-0002-2941-1060

Abbreviations: ADMET, Absorption Distribution Metabolism, Excretion and Toxicity; CHARMm, Chemistry at HARvard Macromolecular Mechanics; DLA, Daltons Lymphoma Ascites; DMBA, dimethylbenz[a]anthracene; DMEM, Dulbecco's Modified Eagle medium; DPPH, 2,2-diphenyl-1-picryl-hydrazyl-hydrate; EAC, Ehrlich Ascites Carcinoma; LC-MS/MS, Liquid Chromatography with tandem Mass Spectrometry; MTT assay, 3-[4,5-dimethylthiazole-2-yl]-2,5-diphenyltetrazolium bromide; PBS, Phosphate buffered saline; ROS, Reactive oxygen species

Curry leaf (*Murraya koenigii* L. Spreng., Rutaceae), is a medicinal plant rich in alkaloids, phenolics, flavonoids, saponins, proteins, sterols and triterpenes[8,9] and used in the *Ayurvedic* preparations. Extensive use of curry leaf based preparations in these traditional medicines to cure different types of cancers has invited the scientific efforts to explore the basis of the anti-cancer potential of this plant[10,11]. The active constituents of curry leaves target disorganized signaling pathways with profound roles in cancer proliferation such as JAK (janus kinase)/STAT (signal transducer and activator of transcription) pathway, PI3K (phosphatidylinositol 3 kinase)/Akt (protein kinase B) pathway and mTOR (mammalian target of rapamycin) pathway, regulating cell growth, proliferation and apoptosis[12]. Many similar studies followed have proven the treatment potential of curry leaf extracts against breast cancer[13], colon cancer[11,14], prostrate cancer[15], cervical cancer[16] and ovarian cancer[17].

Even with all these information, efforts on a systematic attempt to identify the cancer drug molecules from this potential plant is still on. In the present study, we have made an attempt to isolate the antioxidant oleoresin fraction and sub-fractions from curry leaves, identify potential breast cancer drug candidate through chromatographic, spectrometric techniques and *in silico* analyses, to assess the toxicity and antiproliferative potential of drug candidates using *in vitro* cell line studies and to confirm the candidature through induced mouse tumour models and candidate gene expression analyses.

Materials and Methods

Oleoresin extraction

The medium mature and mature leaves from the *in vitro* raised curry leaf plantlets (cv. Suvasini) were used in the study. Oleoresin was extracted from the shade dried and powdered leaves, using Soxhlet apparatus. Ten gram of curry leaf powder was weighed, packed in a coarse filter paper and placed in the extraction chamber of the apparatus. Extraction was carried out using 100% acetone for 9 h till the solvent becomes colourless. After extraction, the extract was transferred to a pre-weighed beaker, kept open for evaporation to remove the traces of acetone, and recorded the final weight of the beaker. Oleoresin recovery (%) was calculated using the following formula:

$$Oleoresin\ recovery\ (\%) = \frac{Weight\ of\ oleoresin}{Weight\ of\ curry\ leaf\ powder}\ x\ 100$$

Antioxidant assay

Potential of the oleoresin in scavenging the reactive oxygen species (ROS) was assessed by DPPH assay, using UV spectrophotometer[18]. Radical scavenging activity was calculated using the following formula:

$$Radical\ scavenging\ activity\ (\%) = \frac{Control\ OD - Sample\ OD}{Control\ OD}\ x\ 100$$

Separation of the antioxidant fraction

Oleoresin with maximum radical scavenging activity was subjected to fraction separation using silica gel column chromatography. The sample was prepared by mixing two grams of the oleoresin extracted from the mature-leaf powder with 20 mL of hexane. Solvent system was prepared using hexane (nonpolar) and ethyl acetate (polar) in the proportions 100:0, 80:20, 60:40, 40:60, 20:80 and 0:100 (hexane: ethyl acetate). The samples were loaded over the top of the packed column and subsequently allowed to move into. Afterwards, the column was filled with 75 mL of 80:20, 60:40, 40:60, 20:80 and 0:100 (hexane: ethyl acetate) and each fraction was collected separately. DPPH assay was performed in each fraction to find out the one with maximum antioxidant activity.

Sub-fractionation and identification of compounds through LC-MS/MS

Fraction with the highest antioxidant activity was sub-fractionated using column chromatography. The fraction was loaded into silica column and subjected to column chromatography. Fractions were collected at five min. interval and a total of 47 fractions were obtained. DPPH assay was done for all the 47 sub-fractions and five sub-fractions with the highest antioxidant activity were identified. Those sub-fractions along with the main fraction were analyzed using LC-MS/MS. The samples were analyzed with Agilent G6550A with triple quadrupole mass spectrophotometer. The samples were mixed with water:acetonitrile in the ratio 95:5 and 3 µL of sample was injected to the machine. Electrospray ionization with positive polarity (ES+) was given at 3500 V capacity voltage, 1000 V nozzle voltage, and gas at 13 L/min. with source temperature 250°C.

Molecular docking

Phytocompounds identified through LC-MS/MS were considered as ligands and docked against breast cancer targets, 17-beta HSD, polo-like kinase 1, exchange protein directly activated by CAMP, NAT-2 receptor, phosphoinotidate-3 kinase, human androgen receptor, dihydrofolate reductase and human estrogen

receptor ligand-binding domain. Interactions were also compared with that of commercial drugs available for cancer viz. fulvestrant, ribociclb, diphenylamine, NSC-54767, tamoxifen, fenritinide and trimetrexate. Structures of the phytocompounds and commercial drugs were retrieved from PubChem and ChemSpider databases. Structures of the cancer targets were retrieved from Brookhaven National Laboratory's database on protein structures.

The 3D structures of the ligands and targets were processed using the protein preparation wizard of Discovery Studio 4.0. Energy minimization of the proteins was done using CHARMm force field. The ligands were filtered as per Lipinski-Veber's protocol. Receptor cavity and Prediction tool has been used to predict the active site of the target protein based on the active amino acid present in the binding site and the docking was done using CDOCKER protocol. The best pose of the phytocompound and the interacting target protein was identified from the minimum difference between C-DOCKER and C-DOCKER interaction energies. The binding affinity of each compound against their targets has been identified (Ligand binding energy = $E_{complex} - E_{ligand} - E_{protein}$) and the scoring function was based on these binding energies. ADMET analysis was done using ADME/T Descriptor algorithm, by which the pharmacokinetic properties such as aqueous solubility, human intestinal absorption, blood brain barrier (BBB) penetration, cytochrome P450 inhibition (CYP2D6) and hepatotoxicity levels were estimated for the successful ligands.

***In vitro* cytotoxicity and anti-proliferative analyses**

The promising molecules identified through molecular docking were tested for their cytotoxicity and anti-proliferative properties. They were purchased in their chemical form (Sigma Aldrich) and used in the analyses. Trypan blue exclusion assay in murine cancer cell lines and MTT assay in human breast cancer cell line were used in cytotoxicity and anti-proliferative studies, respectively. murine cancer cell lines, ehrlich ascites carcinoma (EAC) and daltons lymphoma ascites (DLA) and Human breast cancer cell line, MCF-7 were procured from Amala Cancer Research Centre, Thrissur, India. EAC and DLA were maintained in the peritoneal cavity of the mouse whereas human cell lines were cultured in Dulbecco's modified eagle medium (DMEM), maintained at 37°C in the incubator.

Approximately, 1×10^6 tumour cells of DLA and EAC were incubated in 1 mL PBS (phosphate buffered saline) containing different concentrations of test materials at 37°C for 3 h. The percentage of dead cells was determined by trypan blue exclusion method.

MTT assay is a colorimetric assay which is based on the conversion of yellow dye MTT [3-(4,5-dimethyl-thiazol-2-yl)-2,5-diphenyltetrazolium bromide] into a purple formazon. For MTT assay, the MCF-7 cells were seeded at a density of 5×10^3 cells/ well in 500 µL of the medium in a 24-well culture plate and cultured for 24 h. Then, the cells were treated with 40, 80, 120, 160, 200, 240 and 280 µg/mL of test materials for 24, 48 and 72 h. After treatment, the cells were incubated with 0.5 mg/ mL of MTT at 37°C for 4 h and with DMSO at room temperature for 15 min. The absorbance of the samples was measured at 570 nm on a scanning multi-well spectrophotometer. Percentage of inhibition was calculated as the ratio of the difference in the OD values of the control sample and test sample and the OD value of the test sample. Experiments were performed at least three times, mean±SE was calculated and statistically analyzed using Graph Pad software followed by Dunnetts test, with $P<0.05$* and $P<0.01$** considered significant.

Anticancer efficacy analysis using mouse mammary tumour model

Based on the *in vitro* results, the most promising phytocompound was carried forward to the *in vivo* analyses in mouse mammary tumour model. All the animal experiments were conducted with the approval of the Institutional Animal Ethical Committee, Amala Cancer Research Centre, Thrissur, India, according to the rules and regulations of Committee for the Purpose of Control and Supervision of Experiments on Animals (CPCSEA) constituted by the Animal Welfare Division, Government of India. Thirty-six female Swiss Albino mice (procured from Small Animal Breeding Station, Kerala Veterinary and Animal Sciences University, India) were housed under standard conditions of 24-28°C, 60-70% humidity and 12 h dark/light cycle, and fed with mouse feed and water *ad libitum*.

Acute toxicity study was done to find out the toxic effects of the selected drug. The drug was orally administered at 100 mg/ kg body wt. for one day and monitored for 14 days.

Mammary tumour was induced by the oral administration of dimethylbenz[a]anthracene (DMBA,

20 mg/kg body wt.) in female Swiss albino mice[19]. DMBA was dissolved in sesame oil and given to all the groups of animals once in a week for six weeks. There were six animal groups, each with six mice. Group I: Normal, Group II: control-DMBA treated, Group III: vehicle control-sesame oil, Group IV: tamoxifen (10 mg/kg body wt.), and Group V: drug-low dose and group VI: drug-high dose. Drug selected was also given orally, each day for six weeks. The experimental and control animals were carefully examined daily and sacrificed after the sixth week. Blood and serum were collected for blood tests, liver function test and renal function test. Histopathology of the mammary pad, kidney and liver tissues were performed.

Gene expression analyses

From the mammary pad of the mice, RNA was isolated using TRIzol method and cDNA was prepared (RevertAid First Strand cDNA synthesis kit, ThermoFisher Scientific, India). The qRT-PCR analyses were performed (StepOnePlus™ Real-Time PCR system, ThermoFisher Scientific) using SsoAdvanced Universal SYBR Green Supermix (BioRad) to study the expression profile of the genes, *ER-1*, *Bcl-2*, *c-Myc* and *Pin 1* with reference to the house keeping gene *β-actin*. The primer details are presented in Supplementary Table 1 (*All supplementary data are available only online along with the respective paper at the journal website* (*http://ijeb.res.in*) *as well as NOPR repository at http://nopr.res.in*).

Results

Oleoresin extraction

Medium mature and mature leaves have yielded 7.87 and 9.16% oleoresin, respectively. DPPH assay was conducted on the extracted oleoresin along with the control, butylated hydroxyanisole (BHA). Percent inhibition of ROS was highest for BHA (91.14%) followed by oleoresin extracted from mature leaves (85.19%) and oleoresin extracted from medium mature leaves (83.30 %) (Suppl. Table S2). As oleoresin extracted from mature leaves showed better results, it was used for further studies.

Separation of antioxidant fraction by column chromatography

Oleoresin was separated by column chromatography using a solvent system composed of different concentrations of hexane and ethyl acetate. Yield of the fraction extracted in each solvent system, after complete evaporation of the solvent, is shown in Suppl. Table S3. The highest yield was recorded for the fraction extracted using 60:40 (hexane: ethyl acetate) solvent system (706.4 mg) and the lowest was found in the fraction extracted using 100 percent ethyl acetate (50.6 mg). DPPH assay conducted on each fraction had shown that the standard antioxidant butylated hydroxianisole possess the highest free radical inhibition (91.147%) (Suppl. Table S4). Among the fractions, 60:40 (hexane: ethyl acetate) fraction recorded the highest inhibition of DPPH (88.680 %) followed by 40:60 fraction (85.140%).

The whole fraction of 60:40 (hexane: ethyl acetate) was subjected to sub-fractionation at five min. interval using column chromatography. A total of 47 sub-fractions were collected, evaporated and subjected to DPPH assay. Sub-fractions 26, 28, 34, 38 and 40, collected at 130, 140, 170, 190 and 200 min, respectively have given the highest percent inhibition for DPPH (91.080, 91.510, 91.080, 89.535 and 89.535, respectively) (Suppl. Table S5) and were selected for LC-MS/MS analysis. LC-MS/MS analysis was carried out for the 60:40 hexane:ethyl acetate whole fraction and five sub-fractions. The number and details of compounds identified from these six samples are presented in Suppl. Tables S6 A and B. From each fraction, 100 compounds have been analyzed and a total of 98 compounds were identified.

Molecular docking

Sixty-nine ligands identified through LC-MS/MS, seven FDA approved drugs and eight target proteins for cancer were used in molecular docking studies. Among the ligands, 43 passed the filtering using Lipinski rule and among the cancer drugs, Fulvestrant failed. The docking scores of the selected ligands with the cancer targets are given in Table 1.

Ligand valylmethionine has shown good interaction with the cancer target 17-beta HSD, with minimum deviation between CDOCKER energy and CDOCKER interaction energy (0.0388 kcal/mol) and good binding energy (-66.7903 kcal/mol). Hence, valylmethionine can be used as a drug candidate to target 17-beta HSD. With the target polo like kinase 1 (PLK-1), both valylmethionine and pheniramine had good interaction. Valylmethionine recorded the least deviation between CDOCKER energy and CDOCKER interaction energy and interacted at the critical amino acid (Lys_{82}) of active site of PLK-1. Alpha-aminodiphenylacetic acid and Valylmethionine interacted with EPAC2 at Glu_{404} residue while commercial drug diphenylamine failed to from any

Table 1 — Docking scores for different cancer targets with selected ligands

Type of compound	Ligand	(-) CDOCKER energy (kcal/mol)	(-) CDOCKER interaction energy (kcal/mol)	No. of H bonds	Amino acid bound to H bond	Distance (A^o)	Binding energy (kcal/mol)
Target: 17-beta HSD							
Curry leaf phyto-compound	Valylmethionine	34.9551	34.9939	4	Ser_{12}* Gly_{15}* Asn_{90}* Lys_{159}*	2.02656 2.00665 2.12888 2.07639	–66.7903
	Flucoxetine	23.9072	33.6213	3	Ser_{12}* $Thr_{190}(2)$*	2.07231 1.90962	–26.1875
	Prometon	25.9838	28.5795	1	Ser_{12}*	2.38996	–19.8592
	Alpha-amino diphenylacetic acid	23.1847	30.4697	5	$Lys_{159}(2)$* $Asn_{90}(2)$* Gly_9*	2.37818 1.77962 2.19294	–12.3566
Standard antioxidant	BHA	16.4736	24.9752	3	Gly_{15}* Ser_{12}* Asn_{90}*	1.96752 1.93116 2.03604	–30.114
Commercial drug	Fluvestrant	Failed in Lipinski Veber rule					
Target: Polo-like kinase 1							
Curry leaf phyto-compounds	Valylmethionine	38.9120	40.8400	1	Lys_{82}*	1.98307	–122.5233
	Pheniramine	28.9006	37.2325	1	Ser_{287}*	1.92422	–94.2229
	Alpha-amino diphenylacetic acid	21.8506	27.2960	1	Arg_{136}*	2.07521	–38.8795
	Histidinol	24.4151	25.4601	1	Cys_{133}*	2.23143	–29.6290
Standard antioxidant	BHA	17.5853	28.2903	1	Cys_{133}*	1.93877	–36.4093
Commercial drug	Ribociclib	–1.32815	55.2089	1	Asp_{194}*	2.10157	–73.3288
Target: Exchange protein directly activated by CAMP							
Curry leaf phyto-compounds	Alpha-amino diphenylacetic acid	33.6452	41.6221	2	Gly_{404}* Lys_{489}*	1.81371 1.96444	–153.8738
	Histidinol	22.7564	29.5362	3	His_{781} Thr_{914} Glu_{62}	2.07356	–110.966
	Valylmethionine	12.3313	21.8548	4	Arg_{404}* Lys_{489}*	1.81371 1.96444	–29.2632
Standard antioxidant	BHA	22.1629	30.2810	1	Leu_{406}*	1.99432	–42.9882
Commercial drug	Diphenylamine	19.0380	26.2256	-	-	-	-
Target: NAT-2 receptor							
Curry leaf phyto-compounds	Pheniramine	28.9006	37.2325	1	Ser_{287}*	1.92422	–94.2229
	Alpha-amino diphenylacetic acid	26.9884	31.9594	4	$Ser_{216}(3)$* Thr_{214}*	2.3497 1.91883	–77.8636
	Histidinol	20.5092	27.1549	2	Ser_{287}* Ser_{216}*	2.02809	–56.9825
Standard antioxidant	BHA	20.0084	27.8699	1	Ser_{287}*	1.96362	–47.2294
Commercial drug	NSC-54767	53.2944	59.4875	1	Gly_{104}*	2.4337	–142.4264
Target: Phosphoinositide-3 kinase							
Curry leaf phyto-compounds	Histidinol	23.7478	30.5784	3	$Glu_{880}(2)$* Val_{882}*	2.29569 2.1777	–96.1723
	Pheniramine	22.7752	30.9258	1	Met_{953}*	2.28098	–25.7181
	Doxylamine	22.4484	31.5954	1	Ser_{806}	2.01588	–19.2485
Standard antioxidant	BHA	17.6706	25.5117	-	-	-	-
Commercial drug	Tamoxifen	-					
Target: Human androgen receptor							
Curry leaf phyto-compounds	Histidinol	28.3878	33.2952	3	Thr_{877}* Asn_{705}* Leu_{704}*	1.89568 1.85509 2.03080	–137.0752

(Contd.)

Table 1 — Docking scores for different cancer targets with selected ligands (*Contd*.)

Type of compound	Ligand	(-) CDOCKER energy (kcal/mol)	(-) CDOCKER interaction energy (kcal/mol)	No. of H bonds	Amino acid bound to H bond	Distance (A^o)	Binding energy (kcal/mol)
Standard antioxidant	BHA	25.6846	34.7773	1	Gln_{711}*	2.07177	–37.4466
Commercial drug	Fenretinide	Positive docking energy					
Target: Dihydrofolate reductase (DHFR)							
Curry leaf phyto-compounds	Histidinol	24.4062	28.9232	3	Ile_5* Asp_{27}(2)*	2.08063 1.91422	–61.0572
Standard antioxidant	BHA	18.3893	26.6817	1	Trp_{22}*	2.25661	–46.452
Commercial drug	Trimetrexate	23.2455	57.0153	5	Gly_{15} Ile_5* Ile_{94}* Asp_{27}(2)*	2.22369 1.96387 1.96556 2.25951	–132.5889
Target: Human estrogen receptor ligand-binding domain							
Curry leaf phyto-compounds	Histidinol	22.1024	28.5924	2	Leu_{346}* Glu_{353}*	2.12417 2.22719	–233.3435
Standard antioxidant	BHA	20.7126	30.0847	1	Glu_{353}*	2.00878	–10.8
Commercial drug	Trimetrexate	17.6477	56.9947	1	Asp_{351}*	1.99583	–161.2334

hydrogen bond with the target. Alpha-aminodiphenylacetic acid, pheniramine and histidinol interacted with NAT-2 protein. Alpha-amino-diphenylacetic acid recorded the least difference between CDOCKER and CDOCKER interaction energy and formed three hydrogen bonds with Ser_{216}, amino acid at the active site, which may cause inhibition of the target NAT-2 protein.

With the target phosphoinositide-3 phosphate (PI3K), histidinol and doxylamine have interacted through Glu_{880} and Met_{953} suggesting that the binding of these compounds inhibits PI3K. Only histidinol has interacted with human androgen receptor (AR). It showed high binding energy and interacted with critical amino acids (Thr_{877}, Asn_{705} and Leu_{704}) in the binding site of AR. Surprisingly, the commercial drug fenrtinide had shown a positive CDOCKER energy. Histidinol interacted with the target DHFR at amino acid Ile_5 and Asp_{27} while commercial drug Trimextrexate interacted at Ile_5, Asp_{27} and Ile_{94} with more binding energy than histidinol. With estrogen receptor ligand binding domain, only histidinol has interacted with high docking energy, forming a hydrogen bond with Leu_{346} and Glu_{353}.

ADME/T analysis of ligands

The pharmacokinetic properties of the ligands and approved drugs were studied through ADME/T analysis (Table 2). Based on ADME/T values, ligands and commercial drugs were grouped into Acceptable (A, compounds not in acceptable range for ≤2 parameters), Highly acceptable (HA, compounds satisfy the acceptable range for all parameters) and Non-acceptable (NA, compounds not in acceptable range for ≥3 parameters.).

Among the seven curry leaf ligands which interacted with cancer targets, only two compounds, alpha-amino diphenylacetic acid and valylmethionine, were highly acceptable. They were easily absorbed in body, easily soluble in body fluids, non-inhibitor in action on CYP2D6 drug metabolizing enzyme with less penetration in CNS and exhibited non-toxic effect in liver. Remaining phytocompounds were found acceptable, either too soluble as in histidinol or interfere with CYP2D6 enzyme as in doxylamine. Pheniramine and doxylamine had high penetration in the central nervous system while prometon showed hepatotoxicity. Among the commercial drugs, only trimetrexate was highly acceptable and others were acceptable. Of the eight targets, histidinol interacted with seven targets and was found to be a promising phytocompound with anticancer activity, even though it was too soluble in ADME/T analysis.

Short-term cytotoxicity analysis by Trypan blue exclusion assay

Of the seven phytocompounds that interacted better with the cancer targets, doxylamine, histidinol and pheniramine were tested *in vitro* against breast cancer cell line MCF-7 and murine cancer cell lines DLA and EAC. They were purchased in their chemical form as doxylamine succinate salt, L-histidinol dihydrochloride and pheniramine maleate salt, respectively. Trypan blue exclusion assay, the earliest and widely used method for measuring the viability of the cells, was used to screen the drug candidates. In cases of daltons lymphoma ascites (DLA) and ehrlich

Table 2 — ADME/T properties of ligands from curry leaf interacted against cancer targets and the commercial drugs

Compound Name	PubChem ID	ADMET Solubility level	ADMET Absorption level	ADMET BBB level	Hepatotoxic Prediction	CYP2D6 Prediction
Ligands from curry leaf						
Alpha-amino diphenylacetic acid	18289	3	0	3	FALSE	FALSE
Doxylamine	3162	3	0	1	FALSE	TRUE
Flucoxetine	3386	2	0	0	FALSE	TRUE
Histidinol	776	5	1	4	FALSE	FALSE
Pheniramine	4761	3	0	1	FALSE	FALSE
Prometon	4928	3	0	2	TRUE	FALSE
Valylmethionine	292427	4	0	3	FALSE	FALSE
Commercial drugs						
Diphenylamine	11487	3	0	1	TRUE	FALSE
Fenretinide	5288209	1	1	4	TRUE	FALSE
Fulvestrant	17756771	1	3	4	FALSE	FALSE
NSC-54767	104758	3	3	4	TRUE	FALSE
Ribociclib	44631912	2	0	3	TRUE	FALSE
Tamoxifen	2733526	1	1	0	TRUE	FALSE
Trimetrexate	5583	2	0	4	FALSE	FALSE

Table 3 — Percentage of inhibition of proliferation MCF-7 cells by PMS, DSS and – after 24, 48 and 72 h of treatment

Conc. (µg/mL)	Percentage inhibition of proliferation								
	PMS			DSS			LHD		
	24 h	48 h	72 h	24 h	48 h	72 h	24 h	48 h	72 h
40	4.25±2.2	27.92±2.4***	93.63±3.2***	2.34±0.9	11.26±1.9**	44.96±3.3***	1.06±0.3	1.30±0.2	6.32±0.3
80	5.91±2.5	35.52±3.3***	95.08±2.3***	5.31±0.7	24.07±1.4***	55.56±3.6***	1.49±0.5	2.43±0.6	8.28±0.5
120	30.00±3.4	55.63±2.5***	95.18±2.6***	8.92±0.5	31.82±2.2***	62.89±3.2***	2.55±0.1	4.11±0.7	14.06±0.9
160	32.06±2.7	62.34±2.8***	96.55±3.6***	17.83±1.2	40.69±2.6***	68.99±3.7***	3.18±0.5	6.93±0.5	19.81±1.2
200	37.37±2.1	67.10±3.1***	97.24±3.1***	26.90±1.8	46.32±2.0***	73.38±4.1***	4.25±0.6	7.14±0.2	20.11±1.3
240	37.58±2.5	69.05±3.4***	98.41±4.0***	33.97±1.9	46.75±1.8***	76.92±3.6***	5.31±1.2	12.97±1.3	24.16±1.9
280	38.00±2.2	71.21±2.5***	98.46±3.6***	38.22±1.5	58.23±2.1***	80.49±3.4***	5.94±1.6	14.72±1.5	28.82±1.5

[Mean±SD (n=3) **significant at P <0.01, ***significant at P <0.001]

ascites carcinoma (EAC) cells, the number of dead cells was very low when treated with the drug candidates even at the highest concentration of 400 µg/mL. Only pheniramine maleate salt showed some cytotoxicity with 15 and 10% inhibition on DLA and (EAC) cells, respectively. Since the inhibition observed was less than 50% in all the treatments, it was concluded that these drug candidates have no significant cytotoxicity against murine cancer cells.

Anti-proliferative analysis by MTT assay

The percent inhibition of proliferation (mean±SD) of MCF-7 cells by the drug candidates pheniramine maleate salt (PMS), doxylamine succinate salt (DSS) and L-histidinol dihydrochloride (LHD) is presented in Table 3. Inhibition responses were dose-dependent and based on this, IC_{50} values were calculated.

When MCF-7 was incubated with PMS for 24 h, the maximum inhibition obtained at the concentration of 280 µg/mL was only 38.0±2.2%. At 48 h, maximum inhibition at 280 µg/mL was 71.21±2.5%, with IC_{50} at 108 µg/mL. More than 90% inhibition was seen in all the concentrations of PMS at 72 h with the maximum of 98.46±3.6% at 280 µg/mL, and the corresponding IC_{50} value was 14 µg/mL.

At 24 h of incubation of MCF-7 cells with 280 µg/mL DSS, maximum inhibition obtained was 38.22±1.5%, nearly the same as that obtained with PMS. At 48 and 72 h, maximum inhibition were 58.23±2.1 and 80.49±3.4%, with IC_{50} values of 252 and 61 µg/mL, respectively.

LHD did not inhibit the proliferation of the breast cancer cells. The maximum percentage of inhibition even at 72 h of incubation at 280 µg/mL was 28.82±1.5%.

Per cent inhibition of proliferation of the MCF-7 cells by various concentrations of the drug candidates were compared by two-way ANOVA followed by Dunnett's test. When the responses of PMS after 24 h were compared with that at 48 and 72 h, all concentrations registered significant increase (P <0.001). With time, DSS also had shown significant increase (P <0.001) in all the values, except for 40 µg/mL concentration at 48 h, for which the increase was significant at P <0.01.

Acute toxicity study

Acute toxicity studies were done in Swiss albino mice using a high dose of 100 mg PMS/kg body wt. Monitoring for 14 days after the drug administration

had shown no significant differences in the behavioural and general appearance between the normal and treated groups, indicating that the drug has no toxicity. Hence, $\frac{1}{10}^{th}$ and $\frac{1}{5}^{th}$ of the dose (10 and 20 mg/kg body wt.) were used as low and high doses, respectively.

Anticancer efficacy analysis using mouse tumour model

After six weeks of carcinogen administration, the tumour developed (Fig. 1) and the mice were sacrificed in CO_2 chamber. The average values of uptake of feed, water and changes in the weight of the animal groups over the six weeks are presented in Suppl. Tables S7-S9. Three mice each from each category were used to collect the blood to analyze the haematological parameters and serum for liver function and renal function tests. The mean values for the haematological and biochemical parameters from the liver and renal function tests were recorded and compared with the control.

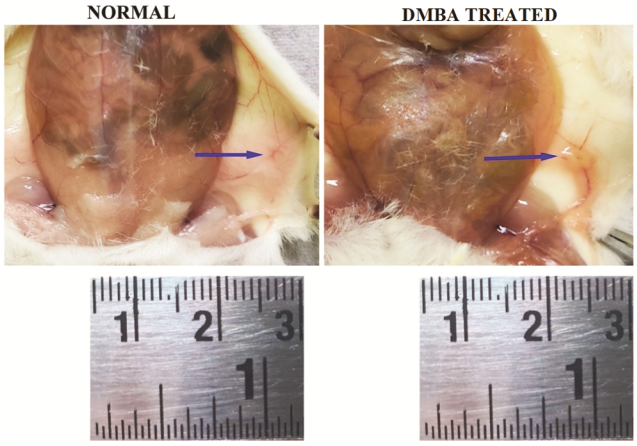

Fig. 1 — Comparison of tumours developed in the mammary pads of the normal and DMBA treated mice (arrow shows mammary pad)

PMS administration significantly reduced the WBC count in the tumour induced mice, with the standard (P <0.001), PMS low dose (P <0.01) and high dose (P <0.01) groups, showing 6800, 8300 and 6300 cells/ cu mm, respectively (Table 4). Tamoxifen treated animals exhibited a significant decrease (P <0.05) in the WBC count compared to the normal and DMBA-treated animals. Variations observed among the different treatments for haemoglobin, platelet count, total RBC count, neutrophils, lymphocytes and eosinophils, were not significant.

In liver function tests, SGOT (Serum glutamic-oxaloacetic transaminase) levels were found to have reduced significantly in the standard and PMS low dose treatments (272 and 303 U/L, respectively). Similarly, for SGPT (Serum glutamic pyruvic transaminase), levels of standard, PMS low dose and PMS high dose were significantly lower (72, 65 and 76 U/L, respectively) than that of the control group (101 U/L).

For ALP (Alkaline phosphatase), levels of standard, PMS low dose and PMS high dose were 146, 73 and 156 U/L, respectively compared to the control groups with 234, 128 and 79 U/L (Table 5). Variations among the treatments for total protein, albumin, globulin, total bilirubin were insignificant.

Table 4 — Haematological parameters of breast tumour induced and normal mice

Haematological parameters	Normal	Control	Vehicle control	Standard	PMSLD	PMSHD
Haemoglobin (g/dL)	14.3±0.2	13.2±0.2	12.9±0.2	11.3±0.1	14.6±0.2	13.9±0.2
Total RBC count (millions/cu mm)	8.2±0.1	8.1±0.2	7.8±0.2	7±0.2	8.5±0.2	8.1±0.1
Platelet count (lakhs/cu mm)	10.9±0.2	10.2±0.2	12.9±0.2	11.1±0.2	9.5±0.2	9±0.1
Total WBC count (cells/cu mm)	5600±205	8600±270	8100±190	6800±230***	8300±510**	6300±550**
Neutrophils (%)	8±3	18±2.8	25±2.5	12±8	16±1.5	20±2.1
Lymphocytes (%)	87±2.5	80±2.2	67±1.7	85±3.2	81±3.1	77±4.2
Eosinophils (%)	5±0.1	2±0.1	8±0.2	3±0.2	3±0.1	3±0.1

[Mean±SD (n=3) in comparison with control group. **significant at P <0.01 and ***significant at P <0.001]

Table 5 — Liver function and renal function tests of breast tumour induced and normal mice

Biochemical parameters	Normal	Control	Vehicle Control	Standard	PMSLD	PMSHD
Liver function tests						
SGOT (U/L)	312±5.3	380±4.8	316±3	272±3.5**	303±8.9**	297±4.3
SGPT (U/L)	60±3.1	101±1.5	68±2.2	72±1.5***	65±4.2***	76±2.5***
Alkaline phosphatase (U/L)	234±2.5	128±2.1	79±4.4	146±7.8***	73±2.5***	156±2.4***
Total protein (g/dl)	7±0.4	8±0.9	8.3±0.8	7.7±2.5	7.1±1.5	7.7±0.5
Albumin (g/dl)	3.4±0.2	3.3±0.2	2.9±0.2	3.1±0.1	3.2±0.1	3.4±0.2
Globulin (g/dl)	3.6±0.2	4.7±0.1	5.4±0.2	4.6±0.2	3.9±0.1	4.3±0.3
Total Bilirubin (mg/dl)	0.3±0.1	0.3±0.1	0.2±0.1	0.2±0.1	0.2±0.1	0.3±0.1
Renal function tests						
Urea (mg/dL)	53 ± 0.6	43±0.9	37±0.5	40±0.7	35±0.4	31±0.3
Creatinine (mg/dL)	0.46±0.02	0.48±0.03	0.45±0.01	0.45±0.02	0.44±0.01	0.47±0.03

[Mean±SD (n=3) in comparison with control group. **significant at P <0.01 and ***significant at P <0.001]

In the renal function test, variations in urea and creatinine levels in all the groups were also insignificant, compared to that of control (53 mg/dL urea and 0.46 mg/dL creatinine).

Histopathology of liver, mammary pad and kidney

The histopathological architecture of mammary pad, liver and kidney of the animals from the six groups were photographed under light microscope (200X). The histology of mammary pads of untreated groups revealed the presence of normal adipose tissue, mammary duct and stromal tissue (Fig. 2). In control and low dose groups, the stroma had shown carcinomatous growth. In high dose treatment group, the tumour size was relatively smaller and tumour initiation and progression were much reduced compared to control groups.

Histopathological examination of liver tissues from the normal group had shown typical hepatic architecture (Fig. 3). The control and low dose treatment groups had cytoplasmic degeneration and aggregation of inflammatory cells, whereas standard group showed hepatocellular injury. High dose treatment group showed less cytoplasmic degeneration.

The histopathology of kidney tissues from the normal group showed normal glomerulus and distal and proximal tubules (Fig. 4). The control and treated

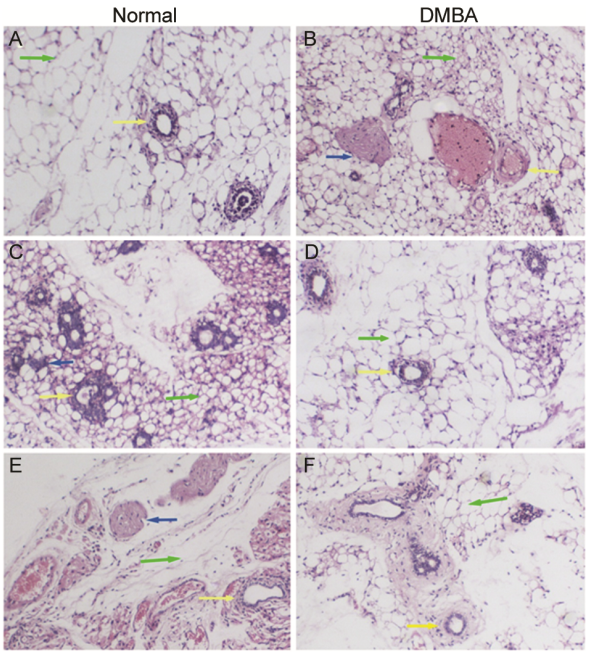

Fig. 2 — Histological section of mammary gland of normal mice and DMBA induced breast cancer mice. (A) normal; (B) control; (C) vehicle control; (D) standard; (E) PMSLD; and (F) PMSHD. yellow arrow: duct; green arrow: adipose tissue; and blue arrow: hyperplastic areas]

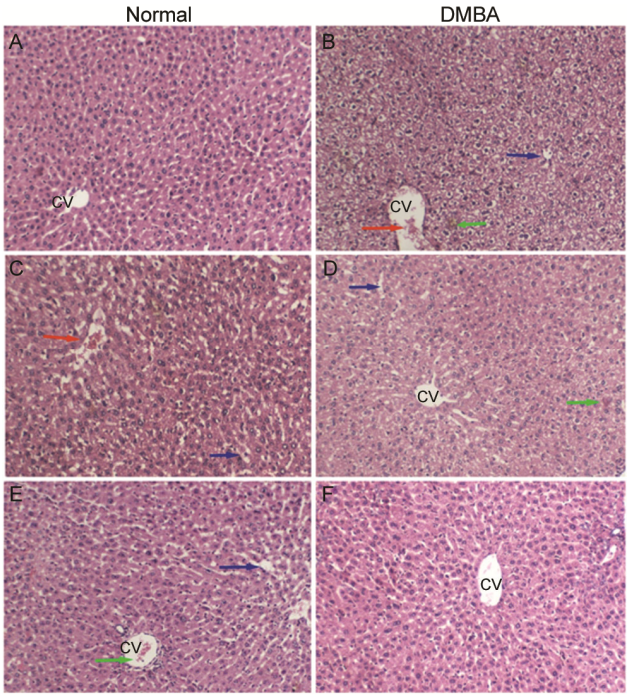

Fig. 3 — Histological section of liver of normal mice and DMBA induced breast cancer mice. (A) normal; (B) control; (C) vehicle control; (D) standard; (E) PMSLD; and (F) PMSHD. [red arrow: infiltration of inflammatory cells; blue arrow: cytoplasmic degeneration; green arrow: necrosis; and CV: central vein]

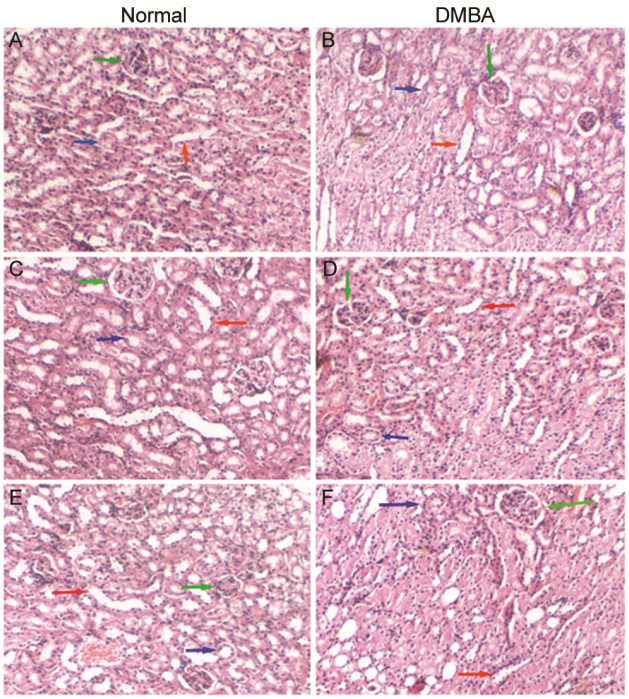

Fig. 4 — Histological section of kidney of normal mice and DMBA mice. (A) normal; (B) control; (C) vehicle control; (D) standard; (E) PMSLD; and (F) PMSHD (green arrow: glomerulus; red arrow: distal tubules; and blue arrow: proximal tubules)

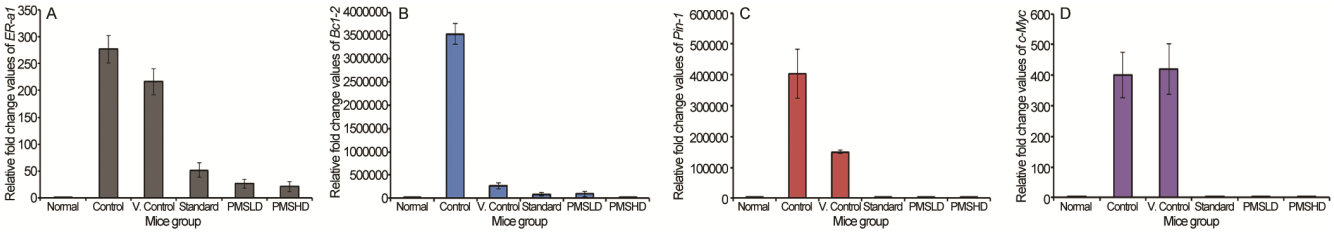

Fig. 5 — Relative expression of the candidate oncogenes A. *ER-α1*, B. *Bcl-2*, C. *Pin-1* and D. *c-Myc* among different treatment groups

groups had no visible differences in their renal architecture.

Expression analysis of candidate oncogenes

From the mice belonging to each treatment, total RNA was isolated, cDNA was prepared and qRT-PCR was done to measure the relative expression of the candidate oncogenes, *ER-α1*, *Bcl-2*, *c-Myc* and *Pin1*, using *β-actin* as the reference gene.

The relative expression of the genes among different treated groups and normal group is shown in the Figs. 5A-D. Fold change values for normal group was 1 with which the fold change in all other groups were calculated. Expression of all the genes were increased in the control and vehicle control groups compared with that of normal. The fold change values for PMSLD and PMSHD were very less compared to that of the control group and almost similar to that of standard. For control group, the fold change in the expression of *ER- α1* was 276.75 while, it was 26.61 for PMSLD and 21.69 for PMSHD. The fold change values for *Bcl-2* gene expression were very high, 3535599.11 for control, 97762.77 for PMSLD and 292.42 for PMSHD. High values of fold change were found in the expression of *Pin1* gene also, 402749.5 for control, 1048.79 for PMSLD and 96.65 for PMSHD. The fold change values for the expression of *c-Myc* were 401.06 for control, 0.99 for PMSLD and 3.95 for PMSHD.

In general, higher level of expression was observed for these genes in the control and vehicle control groups. Relatively lower expression of the oncogenes in PMSLD and PMSHD groups indicates that the drug PMS is efficient to reduce the progress of carcinogenesis.

Discussion

Natural compounds derived from the plants are excellent sources of drugs against cancer. Various phytocompounds have been characterized for their anti-cancerous properties. Few plant derived cancer drugs, such as paclitaxel from *Taxus brevifolia* Nutt., are already available in the market whereas various phytochemicals such as allicin from *Allium sativum*, andrographolide from *Andrographis paniculata*, baicalin from *Scutellaria baicalensis*, curcumin from *Curcuma longa*, genistein from *Glycine max*, Nimbolide from *Azadirachta indica*, resveratrol from *Polygonum cuspidatum*, thymol from *Thymus vulgaris*, withaferin-A from *Withania somnifera*, are reported to possess anti-cancer properties and are in pre-clinical trials for the treatment of cancer[20]. The anticancer activity of curry leaf compounds are identified and validated in this study.

Oleoresin extraction

The oleoresin content in black pepper leaves is reported to increase with maturity, with 1.29% increase in mature leaves compared to the emerging ones[21]. This was found to be true with curry leaf also. The anti-oxidant property of the oleoresin also gets enhanced since the total phenol content increases significantly. The oleoresin extract from mature curry leaves possess a high quantity of total phenols[22].

Separation of antioxidant fraction by column chromatography

Column chromatography is a standard methodology followed to fractionate the secondary metabolites. Researchers have been extensively using the various chromatographic strategies to isolate the carbazole alkaloids from curry leaves[23].

DPPH assay is a widely preferred method for evaluating the antioxidant potential of the plant extracts[23] and butylated hydroxianisole is the standard antioxidant used for the comparison[24]. DPPH inhibition by the sub-fractions was higher than that by the main fraction (60: 40 hexane: ethyl acetate), which might be due to the presence of large number of compounds in the fraction. Individual compound isolated from the curry leaf oleoresin will have higher DPPH inhibition than the total oleoresin[23].

Molecular docking

Of the 69 ligands identified, 43 have passed the Lipinski rule. Selection of active inhibitors was based on low binding energy[25]. The difference of more than

10 between CDOCKER energy and CDOCKER interaction energy for ligand and target protein interaction was unstable, hence neglected. All the ADMET parameters were calculated using standard mathematical formulae[26]. Among the phyto-compounds interacting with cancer targets, alpha-amino diphenylacetic acid and valylmethionine, were highly acceptable and among the commercial drugs, only trimetrexate was highly acceptable. Histidinol interacted with seven of the eight targets studied and hence found promising in cancer treatment, even with its too soluble nature. Solubility of the drugs can be modified by physical and chemical methods and hence efforts can be made to improve its solubility while drug formulation.

Short-term cytotoxicity and Anti-proliferative analyses

The compounds pheniramine, doxylamine and histidinol were selected based on their dock scores against cancer targets polo-like kinase, NAT-2 receptor, phosphoinositide-3 kinase and Human estrogen receptor ligand-binding domain, which are the common targets of breast cancer.

Three phytocompounds in its chemical form, doxylamine succinate salt, L-histidinol dihydro-chloride and pheniramine maleate salt, were tested for their cytotoxicity against the murine cancer cells; Daltons lymphoma ascites (DLA) and Ehrlich ascites carcinoma (EAC), using Trypan blue exclusion assay. In cases of DLA and EAC, the number of dead cells was very low when treated with the drugs even at the highest concentration of 400 µg/mL. Pheniramine maleate salt showed cytotoxicity of 15% in DLA cells and 10% in EAC cells.

In a short-term cytotoxicity study conducted by Bellamakondi *et al*.[27], the methanolic extracts of *Caralluma* species were tested against EAC cells (Ehrlich ascites carcinoma) and the CTC_{50} value ranged between 191.3 ± 0.92 and 291.8 ± 3.17 µM. Inhibition of 50% of the total cells is required to confirm the cytotoxicity action of the drug. Since 50% inhibition was not there in any cases, it was concluded that these three molecules do not have considerable cytotoxicity against murine cancer cells.

Assessment of per cent inhibition of proliferation of MCF-7 cancer cells by PMS, DSS and LHD by *in vitro* MTT assay had shown that PMS and DSS inhibit the cancer cell proliferation up to 98.46%. When Kumar *et al*.[28] have tested the anticancer potential of ethanolic extract and essential oil of *Syzygium aromaticum* L. in MCF-7 breast cancer cell lines, IC_{50} values of ethanolic extract were 61.29 and 16.71 µg/mL for 24 and 48 h incubation, respectively. The essential oil achieved IC_{50} at 36.43 and 17.6 µg/mL in 24 and 48 h, respectively. Compared to this, the concentration required for both PMS and DSS to achieve 50 % inhibition at 48 hours of inhibition was higher (108 and 252 µg/mL, respectively) but with 72 h incubation, IC_{50} values were only 14 µg/mL for PMS and 21 µg/mL for DSS. Similarly, Urdiales *et al*.[29] have tested the effects of chlorpheniramine on the activity of ornithine decarboxylase (ODC) enzyme in cultured Ehrlich carcinoma cells and found that the ODC enzyme activity decreased with increase in drug concentration. Among the PMS and DSS lines, PMS performed better as it had lower IC_{50} compared to that of DSS. Hence, PMS was selected for the *in vivo* analysis.

Acute toxicity study

Swiss albino mice were selected for the animal model study as the development of tumour and its metastasis was similar to that of human. Acute toxicity studies were done to find whether the selected drug impose any sort of toxicity in the animals. In order to study the anti-histaminic effect of *Bauhinia racemosa* leaves, Nirmal *et al*.[30] had used 10 mg/kg b.wt. of pheniramine maleate as a standard in male albino mice. Similar quantity of pheniramine maleate salt was administered in various other studies[31]. Hence, a high-dose of 100 mg/ kg body wt. of the drug PMS was administered once to the animals and monitored for 14 days for the changes in the behavioural and general appearance.

Anticancer efficacy analysis using mouse tumour model

PMS administration has significantly reduced the WBC count in the tumour induced mice. Zingue *et al*.[32] has shown that DMBA treatment increases the WBC count significantly compared to that in normal mice.

Liver function test is used to detect damage and inflammation of the liver by analysing the enzymes such as serum glutamic-oxaloacetic transaminase (SGOT), serum glutamic pyruvic transaminase (SGPT) and alkaline phosphatase (ALP). A significant reduction in SGPT, SGOT and ALP levels was observed in the treated mice than that of the normal mice. Reduced level of these serum enzymes indicate the hepato-protective activity of the drug candidate. Similar kind of hepato-protective activity of *Cyathea gigantea* was observed by Kiran *et al*.[33] in paracetamol-induced Wistar albino rats.

Histopathology of liver, mammary pad and kidney

Histopathology, a routine method in cancer diagnosis, provides an insight into the architecture of the tissues in which the disease is manifested. Comparing the tissue slides of mice among different groups helps in inferring the effects of the drug. In this study, histopathological examinations of mammary pad, liver and kidney were carried out. Histopathological analysis of the mammary pad and liver tissues between normal and DMBA treated animal groups indicated that DMBA altered the normal architecture of the tissues. Treatment with PMS at high dose has produced significant changes in the tissue morphology of the DMBA treated animals. The identifiable changes suggest the definite roles of the drug candidate in cell proliferation and organization. Under chronic conditions, lower doses of the drug is reported to produce promising effects compared to the higher doses[34].

Counts on haemoglobin, total RBC, platelet, total WBC, neutrophils, lymphocytes and eosinophils were made under the haematological analyses. A reduction in the RBC count implicated that there is reduction in the transport of oxygen and carbon dioxide. WBCs are involved in defending the body from the foreign agents. Reduction in WBC count implied the destruction of immune system and the animal becomes highly prone to infection. An increase in WBC count suggested enhanced production of antibodies and better resistance to infections. Platelets are involved in blood clotting and a decrease in their concentration suggests a prolonged process of blood clotting and excess blood loss[35].

Liver function test is used for the detection of damage and inflammation of the liver by analysing the liver enzymes such as serum glutamic-oxaloacetic transaminase (SGOT), serum glutamic pyruvic transaminase (SGPT) and alkaline phosphatase. High levels of these enzymes suggested liver damage. Other biochemical parameters included total protein, albumin, globulin and bilirubin. Higher values of bilibrubin, albumin and globulin indicated liver or bile duct problems.

Renal function test included urea and creatinine, levels of which reflected the glomerular filtration rate (GFR). Renal failure is often associated with elevated urea and creatinine.

Two way ANOVA was performed for the test results, with reference to the control group. A significant reduction in the WBC count was found in the standard (P <0.001), PMS low dose (P <0.01) and PMS high dose (P <0.01) groups with values of 6800±230 cells/cu mm, 8300±510 cells/cu mm and 6300±550 cells/cu mm, respectively. In a study conducted by Zingue *et al.*[32], there was a significant increase (P <0.001) in white blood count of the rats treated with DMBA than that of normal ones. Tamoxifen treated animals exhibited a significant decrease (P <0.05) in the WBC count compared with that of normal and DMBA-treated animals. It implicated that WBC count increases when there is a tumour growth or inflammation. Hence, the reduction in the WBC count in the PMS treated groups is promising. Other parameters *viz.* haemoglobin, platelet count, total RBC count, neutrophils, lymphocytes and eosinophils were insignificant. In liver function test, there was a significant reduction in SGOT (serum glutamic-oxaloacetic transaminase) level (P <0.01 for standard and PMS low dose), SGPT (serum glutamic pyruvic transaminase) level (P <0.001 for standard, PMS low dose and PMS high dose) and ALP (alkaline phosphatase) level (P <0.001 for standard, PMS low dose and PMS high dose). Higher levels of SGPT, SGOT and ALP indicated liver cell injury. Since these parameters were lower in the animal groups treated with the drug candidates, on par with the standard, the drug candidates are shown to have effect on the tumour induced animals.

Expression analysis of candidate oncogenes

All the genes analyzed were oncogenes with profound roles in breast cancer. The *ER*-(Estrogen receptor-α) signaling plays a major role in the breast cancer proliferation. It promotes the expression of other oncogenic proteins such as cyclin-D and c-Myc and inhibits the expression of cell cycle inhibitors such as P21[36]. The standard drug tamoxifen is a modulator of *ER-α*. In DMBA induced Wistar albino rats, the *ER-α* activity is reported to have down regulated by *Graviola*[37].

The *Bcl-2* is an anti-apoptotic gene and prognostic marker in breast cancer. The higher expression of this protein is shown to help the cancer cells evade apoptosis. Extract of *Taraxacum officinale* on DMBA induced Wistar rats resulted in a reduced expression of *Bcl-2* gene[38]. The *c-Myc* codes for a pleiotropic transcription factor, upregulated by *ER-α*. Simvastatin treatment is shown to reduce the *c-Myc* expression compared to the control mice receiving only DMBA[39]. The level of *Pin1* protein has role in deciding the transcription of cyclin D1, another

oncogene of breast cancer. Overexpression of *Pin1* activates the promoter of cyclin D1. Also, *Pin1* is shown to modulate the chemo-resistance by upregulating FoxM1 and involved in Wnt/β-catenin signaling pathway[40]. Kim *et al*.[41] showed that amurensin G from *Vitis amurensis* could inhibit angiogenesis of tamoxifen-resistant cancer by inhibiting the expression of *Pin1*.

Through comparative C_T method[42], the fold change in the expression of these genes in the tumour cells were assessed in each animal group. Relatively lower expression of the oncogenes in PMSLD and PMSHD groups indicated that the PMS is a promising drug to reduce the carcinogenesis.

Conclusion

Though curry leaf is known to have activity against breast cancer, potential of individual molecules has not been validated until now. This work details the identification of pheniramine maleate salt, the chemical derivative of pheniramine, as a potential breast cancer drug candidate from curry leaf. Protocols and results in extraction and fractionation of the antioxidant principles from curry leaves, their characterization using LC-MS/MS, identification of molecules with anticancer properties through molecular docking, *in vitro* antiproliferative analysis, *in vivo* studies using mouse breast cancer tumour model and expression analysis of candidate oncogenes, leading to the identification of the drug candidate, are detailed. PMS suppresses the expression of the oncogenes, thus reducing the progression of cancer. In gene expression analyses, action of PMS was comparable with the standard drug, thereby emphasizing its potential.

Acknowledgement

This work was funded by Department of Biotechnology (DBT), Ministry of Science and Technology, Government of India.

Ethical approval

This study was conducted with the approval of the Institutional Animal Ethical Committee, Amala Cancer Research Centre, India (No. ACRC/IAEC/21(2)-P15 dtd.19.11.2021), according to the rules and regulations of the Committee For The Purpose of Control and Supervision of Experiments on Animals (CPCSEA) constituted by the Animal Welfare Division, Government of India.

Conflict of Interest

Authors declare no competing interests.

References

1 Siegel RL, Miller KD, Wagle NS & Jemal A, Cancer statistics, 2023. *CA Cancer J Clin*, 73 (2023) 17.

2 American Cancer Society. *Cancer Facts & Figures 2023*. American Cancer Society, Atlanta (2023) p 84. [https://www.cancer.org/content/dam/cancer-org/research/cancer-facts-and-statistics/annual-cancer-facts-and-figures/2023/2023-cancer-facts-and-figures.pdf].

3 Sathishkumar K, Chaturvedi M, Das P, Stephen S & Mathur P, Cancer incidence estimates for 2022 & projection for 2025: result from National Cancer Registry Programme, India. *Indian J Med Res*, 156 (2023) 598.

4 Sun X, Zhang Y, Li H, Zhou Y, Shi S, Chen Z, He X, Zhang H, Li F, Yin J & Mou M, DRESIS: the first comprehensive landscape of drug resistance information. *Nucleic Acids Res*, 51 (2023) D1263.

5 Duan C, Yu M, Xu J, Li BY, Zhao Y & Kankala RK, Overcoming cancer Multi-drug Resistance (MDR): Reasons, mechanisms, nanotherapeutic solutions, and challenges. *Biomed Pharmacother*, 162 (2023) 114643.

6 Wang N, Ma T & Yu B, Targeting epigenetic regulators to overcome drug resistance in cancers. *Signal Transduct Target Ther*, 8 (2023) 69.

7 Hussan KPS, Thekkekara DB, Pareeth CM, Greena J, Mathew D & Thayyil MS, Antioxidant activity of Erlotinib and Gefitinib: Theoretical and experimental insights. *Free Radic Res*, 56 (2022) 196.

8 Wadanambi PM, Jayathilaka N & Seneviratne KN, A computational study of carbazole alkaloids from *Murraya koenigii* as potential SARS-CoV-2 main protease inhibitors. *Appl Biochem Biotechnol*, 195 (2023) 573.

9 Balakrishnan R, Vijayraja D, Jo SH, Ganesan P, Su-Kim I & Choi DK, Medicinal profile, phytochemistry, and pharmacological activities of *Murraya koenigii* and its primary bioactive compounds. *Antioxidants*, 9 (2020) 101.

10 Noolu B, Ajumeera R, Chauhan A, Nagalla B, Manchala R & Ismail A, *Murraya koenigii* leaf extract inhibits proteasome activity and induces cell death in breast cancer cells. *BMC Complement Altern Med*, 13 (2013) 7.

11 Arun A, Patel OP, Saini D, Yadav PP & Konwar R, Anti-colon cancer activity of *Murraya koenigii* leaves is due to constituent murrayazoline and O-methylmurrayamine A induced mTOR/AKT downregulation and mitochondrial apoptosis. *Biomed Pharmacother*, 93 (2017) 510.

12 Aniqa A, Kaur S & Sadwal S, A review of the anti-cancer potential of *Murraya koenigii* (Curry tree) and its active constituents. *Nutr Cancer*, 74 (2022) 12.

13 Hu G, Pu J, Wang Q & Zou X, Mahanimbine suppresses the proliferation of lung cancer A549 cells via inducing intrinsic apoptotic pathway. *Rev Bras Farmacogn*, 33 (2023) 384.

14 Roshni K, Younis M, Ilakkiyapavai D, Basavaraju P & Puthamohan VM, Anticancer activity of biosynthesized silver nanoparticles using *Murraya koenigii* leaf extract against HT-29 colon cancer cell line. *J Cancer Sci Ther*, 10 (2018) 72.

15 Kamalidehghan B, Ghafouri-Fard S, Motevaseli E & Ahmadipour F, Inhibition of human prostate cancer (PC-3) cells and targeting of PC-3-derived prostate cancer stem

cells with koenimbin, a natural dietary compound from *Murraya koenigii* (L) Spreng. *Drug Des Devel Ther*, 12 (2018) 1119.
16 Amna U, Halimatussakdiah H, Wahyuningsih P, Saidi N, Nasution R & Astryna SY, Phytochemical screening and *in vitro* cytotoxic activity of hexane extract of temurui (*Murraya koenigii* (Linn.) Spreng) leaves against human cervical cancer (HeLa) cell line. *IOP Conf Ser: Mater Sci Eng*, 523 (2019) 012018.
17 Satyavarapu EM, Sinha PK & Mandal C, Influence of geographical and seasonal variations on carbazole alkaloids distribution in *Murraya koenigii*: deciding factor of its *in vitro* and *in vivo* efficacies against cancer cells. *Biomed Res Int*, 2020 (2020) 7821913.
18 Shimada K, Fujikawa K, Yahara K & Nakamura T, Antioxidative properties of xanthan on the autoxidation of soybean oil in cyclodextrin emulsion. *J Agric Food Chem*, 40 (1992) 945
19 Minari JB, Chemopreventive effect of *Annona muricata* on DMBA-induced cell proliferation in the breast tissues of female albino mice. *Egypt J Med Hum Genet*, 15 (2014) 327.
20 Choudhari AS, Mandave PC, Deshpande M, Ranjekar P & Prakash O, Phytochemicals in cancer treatment: From preclinical studies to clinical practice. *Front Pharmacol*, 10 (2020) 1614.
21 Mathai CK, Kumaran PM & Chandy KC, Evaluation of commercially important chemical constituents in wild black pepper types. *Plant Foods Hum Nutr*, 30 (1980) 199.
22 Verma R, Singh N, Tomar M, Bhardwaj R, Deb D & Rana A, Deciphering the growth stage specific bioactive diversity patterns in *Murraya koenigii* (L.) Spreng. using multivariate data analysis. *Front Plant Sci*, 13 (2022) 963150.
23 Sampath SNTI, Jayasinghe S, Attanayake AP, Karunaratne V, Yaddehige ML & Watkins DL, A new dimeric carbazole alkaloid from *Murraya koenigii* (L.) leaves with α-amylase and α-glucosidase inhibitory activities. *Phytochem Lett*, 52 (2022) 87.
24 Weragama D, Weerasingha V, Jayasumana L, Adikari J, Vidanarachchi JK & Priyashantha H, The physicochemical, microbiological, and organoleptic properties and antioxidant activities of cream cheeses fortified with dried curry leaves (*Murraya koenigii* L.) powder. *Food Sci Nutr*, 9 (2021) 5774.
25 Mathew D, John PL, Manila TM, Divyasree P & Rajan VTKS, Therapeutic molecules for multiple human diseases identified from pigeon pea (*Cajanus cajan* L. Millsp.) through GC-MS and molecular docking. *Food Sci Hum Wellness*, 6 (2017) 202.
26 Saakre M, Mathew D & Ravisankar V, Perspectives on plant flavonoid quercetin-based drugs for novel SARS-CoV-2. *Beni-Suef Univ J Basic Appl sci*, 10 (2021) 21.
27 Bellamakondi PK, Godavarthi A, Ibrahim M, Kulkarni S, Naik RM & Maradam S, *In vitro* cytotoxicity of *Caralluma* species by MTT and trypan blue dye exclusion. *Asian J Pharm Clin Res*, 7 (2014) 17.
28 Kumar PS, Febriyanti RM, Sofyan FF, Luftimas DE & Abdulah R, Anticancer potential of *Syzygium aromaticum* L. in MCF-7 human breast cancer cell lines. *Pharmacognosy Res*, 6 (2014) 350.
29 Urdiales JL, Matés JM, de Castro IN & Sánchez-Jiménez FM, Chlorpheniramine inhibits the ornithine decarboxylase induction of Ehrlich carcinoma growing *in vivo*. *FEBS Lett*, 305 (1992) 260.
30 Nirmal SA, Dhasade VV, Laware RB, Rathi RA & Kuchekar BS, Antihistaminic effect of *Bauhinia racemosa* leaves. *J Young Pharm*, 3 (2011) 129.
31 Yuvanc E, Tuglu D, Ozan T, Kisa U, Balci M, Batislam E & Yilmaz E, Investigation of the antioxidant effects of pheniramine maleate and nebivolol on testicular damage in rats with experimentally induced testis torsion. *Acta Cir Bras*, 33 (2018) 125.
32 Zingue S, Njuh AN, Tueche AB, Tamsa J, Tchoupang EN, Kakene SD, Sipping MTK & Njamen D, *In vitro* cytotoxicity and *in vivo* antimammary tumor effects of the hydroethanolic extract of *Acacia seyal* (Mimosaceae) stem bark. *BioMed Res Int*, 2018 (2018) 2024602.
33 Kiran PM, Raju AV & Rao BG, Investigation of hepatoprotective activity of *Cyathea gigantea* (Wall. ex. Hook.) leaves against paracetamol–induced hepatotoxicity in rats. *Asian Pac J Trop Biomed*, 2 (2012) 352.
34 Dimmitt SB & Stampfer HG, Low drug doses may improve outcomes in chronic disease. *Med J Aust*, 191 (2009) 511.
35 Mageed AH, Faraj SA & Maleek MI, A Comparative study of hematological and biochemical parameters in leukemia patients and healthy persons. *HIV Nursing*, 23 (2023) 1599.
36 Mauro L, Pellegrino M, Giordano F, Ricchio E, Rizza P, De Amicis F, Catalano S, Bonofiglio D, Panno ML & Andò S, Estrogen receptor-α drives adiponectin effects on cyclin D_1 expression in breast cancer cells. *FASEB J*, 29 (2015) 2150.
37 Zeweil MM, Sadek KM, Taha NM, El-Sayed Y & Menshawy S, Graviola attenuates DMBA-induced breast cancer possibly through augmenting apoptosis and antioxidant pathway and downregulating estrogen receptors. *Environ Sci Pollut Res*, 26 (2019) 15209.
38 Nassan MA, Soliman MM, Ismail SA & El-Shazly S, Effect of *Taraxacum officinale* extract on PI3K/Akt pathway in DMBA-induced breast cancer in albino rats. *Biosci Rep*, 38 (2018) BSR20180334.
39 Karimi B, Ashrafi M & Masoudian M, Effect of simvastatin on *c-myc*, *cyclin D1* and *p53* expression in DMBA-induced breast cancer in mice. *Physiol Pharmacol*, 24 (2020) 152.
40 Wang T, Liu Z, Shi F & Wang J, Pin1 modulates chemo-resistance by up-regulating FoxM1 and the involvements of Wnt/β-catenin signaling pathway in cervical cancer. *Mol Cell Biochem*, 413 (2016) 179.
41 Kim JA, Kim MR, Kim O, Phuong NTT, Yoon J, Oh WK, Bae K & Kang KW, Amurensin G inhibits angiogenesis and tumor growth of tamoxifen-resistant breast cancer via *Pin1* inhibition. *Food Chem Toxicol*, 50 (2012) 3625.
42 Schmittgen TD & Livak KJ, Analyzing real-time PCR data by the comparative C_T method. *Nat Protoc*, 3 (2008) 1101.